JCTC Journal of Chemical Theory and Computation

Molecular Dynamics of Methyl Viologen-Cucurbit[*n*]uril Complexes in Aqueous Solution

Musa I. El-Barghouthi,*,† Khaleel I. Assaf,† and Abdel Monem M. Rawashdeh*,‡

Department of Chemistry, The Hashemite University, P.O. Box 150459, Zarqa 13115, Jordan, and Department of Chemistry, Yarmouk University, Irbid 21163, Jordan

Received November 23, 2009

Abstract: In this work, molecular dynamics (MD) simulations have been used to study the dynamics of the inclusion complexes of methyl viologen (MV) with cucurbit[*n*]uril, CB*n* (where $n = 6$, 7, and 8) in aqueous solution. The obtained MD trajectories were analyzed and post-processed using the Molecular Mechanics-Poisson−Boltzmann Surface Area (MM-PBSA) method to shed some light on the host−guest intermolecular forces that play a significant role in the formation of the CB inclusion complexes. MV exhibits partial inclusion into CB6 cavity, while deep inclusion was observed for the larger macrocyclic hosts with the two cationic groups interacting with the carbonyl portals. The extracted snapshots reveal an increase in the macrocycle distortion of CB6 and CB7 upon inclusion of the guest molecule. MM-PBSA calculations indicate that CB7 forms the most stable complex with MV. The host−guest electrostatic interactions are the dominant contribution to the complex stability. Furthermore, van der Waals interactions add significantly to the complex binding free energy. The Potential of Mean Force (PMF) for the host−guest distance was obtained by umbrella sampling. No energy barriers were obtained for the guest movement inside the host cavity except in the case of CB6.

Introduction

Cucurbit[*n*]urils (CB*n*) are macrocyclic molecules consisting of *n* number of glycouril repeated units forming symmetric barrel-shaped structures with two oxygen-crowned portals and a hydrophobic interior.[1−5] Due to these structural features, CBs form inclusion complexes with a variety of guest molecules. CB6 was the first member synthesized in 1905 by Behrend et al.,[6] yet the supramolecular chemistry of CB6 was not launched until the 1980s and 1990s. Other sizes of Cucurbiturils, CB5, CB7, CB8, and CB10, were prepared and made commercially available.[7−9] CBs have been explored as supramolecular catalysts, and they play an important role in the construction of polyrotaxanes[10] and supramolecular switches,[11] the removal of contaminants such as colorants from water,[12] and in the pharmaceutical field.[13]

Many experimental studies were performed to examine the inclusion complexation of different types of molecules with CBs.[14−23] One of the guest molecules that showed strong binding with CB host molecules is methyl viologen (MV), a dication molecule, and hence it received great attention. Ong et al. also studied the complexation of an MV guest molecule with CB7. The obtained ^{1}H NMR spectra showed that CB7 forms stable 1:1 inclusion complexes with the guest molecule in aqueous solution. The binding constant was measured by electronic absorption spectroscopy and was found to be 1.0×10^5 M^{-1}. The smaller host CB6 was also found to bind with MV but with a lower binding constant (20 M^{-1}). On the basis of their ^{1}H NMR data, they described the complex as partial inclusion of MV into a CB6 cavity.[24] The interactions between CB7 with MV showed that a 1:1 host−guest complex in an aqueous solution was evidenced by ^{1}H NMR and mass spectroscopy with a high binding constant of 2.0×10^5 M^{-1}, in contrast to β-cyclodextrin which shows a formation constant of about zero. This strong binding was explained by the favorable ion−dipole interac-

* Corresponding author e-mail: musab@hu.edu.jo (M.I.E.-B.), rawash@yu.edu.jo (A.M.M.R.).

† The Hashemite University.

‡ Yarmouk University.

10.1021/ct900622h
Published on Web 03/19/2010

tions between the positive charges of the guest and the portal oxygen atoms of CB7 in addition to the hydrophobic effect inside the cavity.[25] Moon and Kaifer studied the host−guest interactions between CB7 and a series of dialkyl viologens by ^{1}H NMR spectroscopy. The results showed two modes of inclusion, one with short-chain viologenes, which showed inclusion for the aromatic group, and one with long-chain viologens, which showed inclusion of the terminal alkyl groups into the inner cavity of the host.[26] Recent studies have shown that CB8 forms 1:2 (guest/host) and even possibly a 1:3 inclusion complex with *N*,*N*′-dialkyl-viologens when the alkyl chain consists of more than four carbon atoms, while it forms 1:1 for the shorter chains. MV was shown to form a 1:1 complex with a 2.7×10^4 M^{-1} binding constant.[27] Other studies have reported a value of 1.1×10^5 M^{-1} for the binding constant of CB8 with MV.[28]

In this work, the inclusion complexation of MV with CB6, CB7, and CB8 in water will be explored using MD simulation techniques. MV is selected in this study as a model guest molecule due to the availability of numerous experimental data regarding its complexation with several CB hosts, including binding constants and complex geometries. The corresponding MD trajectories will be analyzed to measure the effect of CB cavity size on the inclusion process as well as to gain detailed information on the guest dynamics inside the CB cavity. The flexibility and the distortion of the CB macrocycle in the presence and absence of the guest molecule will be addressed. The Molecular Mechanics−Poisson−Boltzmann Surface Area (MM-PBSA) method will be used to estimate the binding free energy of each CB*n* complex. The components of the binding free energies will also be estimated and used to explore the type of host−guest interactions responsible for complex formation, which may provide further insights into the inclusion phenomenon. The variation of the free energy values or Potential of Mean Force (PMF) with the host−guest distance will be employed by means of the umbrella sampling method to understand more about the energy barriers that may exist during the inclusion process.

Computational Methods

The X-ray structures of CB6, CB7, and CB8 were used as initial geometries.[5,7] The geometry optimization and electrostatic potential of the guest molecule were computed using *ab initio* HF/6-31G* calculations using the Gaussian 03W package.[29] The atomic charges for the guest molecule reproducing these electrostatic potentials were obtained using the RESP methodology,[30] whereas AM1-BCC charges were used for CB*n*.[31] The AMBER 8 software[32] was used throughout this work using the general force field parameter sets.[33] Each system was solvated by a cubic box of TIP3P water molecules with a closeness parameter of 10 Å.[34] Cl^- anions were added when needed to neutralize the system. Periodic boundary conditions were adopted, and the Particle Mesh Ewald method (PME) was used for the treatment of long-range electrostatic interactions.[35] The nonbonded cutoff was set to 10.0 Å. Energy minimization was performed for each solvated complex using the conjugate gradient algorithm, heated up to 298 K for 60 ps, and followed by 200 ps equilibration at 298 K and 1 atm. Production runs were carried out for 5 ns; the system was coupled in the NPT ensemble to a Berendsen thermostat at 298 K and a barostat at 1 atm. A 2 fs time step with a saving of the structure every 2 ps was used, and the nonbonded pair list was updated every 25 steps.

Analysis of the obtained MD trajectories was conducted using the PTRAJ module of AMBER. For hydrogen bond analysis, a hydrogen bond cut distance $\leq$ 3.0 Å and angle $\geq$ 120° were used. Visualization of the obtained trajectories was done using the VMD program.[36]

For MM-PBSA calculations, 2500 snapshots of the unbound guest molecule, CB*n*, and their complexes were taken from their independent MD trajectories. The explicit water molecules and the added ions were removed in each snapshot. Details on estimating the binding free energy ΔG_{bind} and its components are described below.

The binding free energy ΔG_{bind} was estimated as follows:

$$\Delta G_{bind} = \Delta E_{gas} + \Delta G_{solv} - T\Delta S \quad (1)$$

where ΔE_{gas} is the interaction energy between the guest and host in the gas phase and is given by

$$\Delta E_{gas} = \Delta E_{INT} + \Delta E_{elect} + \Delta E_{vdW} \quad (2)$$

where ΔE_{INT} is the change in the internal energy upon complexation. ΔE_{elect} and ΔE_{vdW} represent the host−guest electrostatic and van der Waals interactions, respectively.

The solvation free energy ΔG_{solv} was estimated as the sum of electrostatic solvation free energy ΔG_{PB} and apolar solvation free energy ΔG_{NP}:

$$\Delta G_{solv} = \Delta G_{PB} + \Delta G_{NP} \quad (3)$$

ΔG_{PB} is computed in a continuum solvent using the PBSA program of AMBER 8, while the ΔG_{NP} was calculated from the solvent-accessible surface area (SASA), which was estimated by the MSMS program using a probe radius of 0.14 nm,[37] which is given by

$$\Delta G_{NP} = \gamma \cdot \mathrm{SASA} + b \quad (4)$$

where $\gamma = 0.00542$ kcal/(mol Å^2) and $b = 0.92$ kcal/mol.

The change of the solute entropy upon complexation, $T\Delta S_{conf}$, was estimated from normal-mode analysis using the NMODE module of the AMBER 8 program.

Since prediction of the solute configurational entropy contribution ($T\Delta S_{conf}$), computed by the normal-mode analysis of the NMODE module in the AMBER 8, is associated with a relatively large error,[38,39] two values of the binding free energies of the complexation process were calculated in this work: ΔG, which is the complexation free energy excluding the solute configurational entropy contribution ($T\Delta S_{conf}$), and ΔG^*, which includes the solute configurational entropy contribution ($T\Delta S_{conf}$). Potentials of mean force, PMF, were generated for the inclusion of the guest molecule into the host cavity. The reaction coordinate used in the umbrella sampling was the distance (r) between the methyl carbon atom attached to the nitrogen atom (dark spot) in MV and the center of mass of one CB carbonyl portal (gray portal), as shown in Figure 1. The values of r ranged from

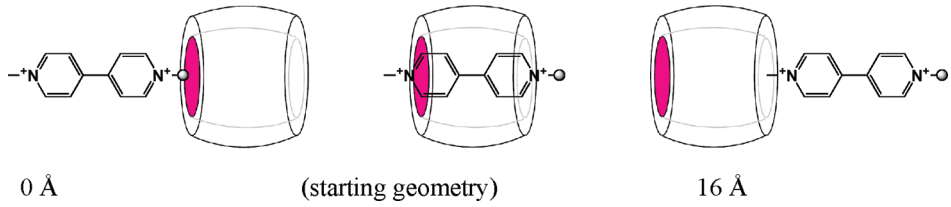

Figure 1. Definition of the distance used in umbrella sampling.

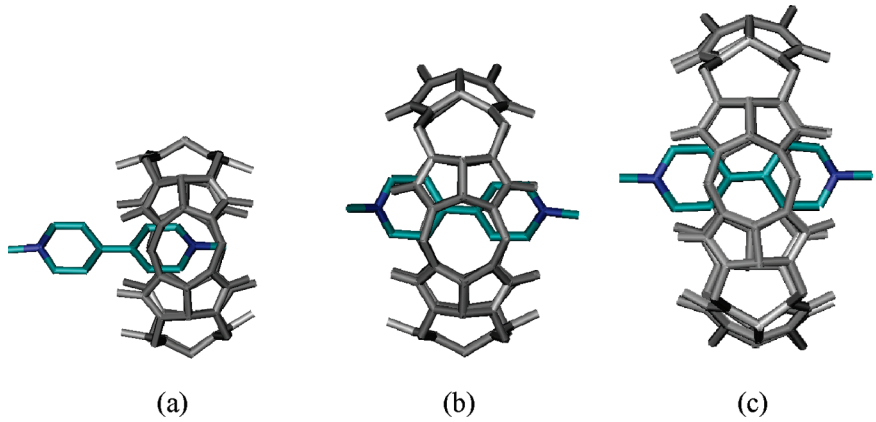

Figure 2. Average structures of the studied complexes, (a) CB6/MV, (b) CB7/MV, (c) CB8/MV.

0 to 16 Å in 1.0 Å intervals. The initial distance corresponds to the inclusion of the guest molecule for CB7 and CB8, while it corresponds to the partial inclusion of the guest in the CB6 cavity. Then, the distance was varied to pull out the guest molecule from each rim of CB. Umbrella potential with a force constant of 6 kcal/mol/Å^2 for each position was applied. Each biasing MD simulation consists of an equilibrium run of 260 ps using a protocol similar to the conventional MD simulations described above, followed by a production run of 500 ps. The distance data for each simulation were collected in 5.0 fs intervals. The results were post-processed using the Weighted Histogram Analysis Method (WHAM).[40,41]

Results and Discussion

Five-nanosecond MD simulations for CB6, CB7, and CB8 and their 1:1 complexes with MV were performed in water to study the dynamics of the host and guest molecules and the intermolecular forces responsible for the complex formation.

The average structures of the corresponding 1:1 complexes obtained from the 5 ns MD trajectories of the complexes are shown in Figure 2. The average structure of CB6/MV showed a partial inclusion of MV into the cavity, where one of the pyridinium rings was located inside the cavity while the other ring interacted with the surrounding water molecules. On the other hand, the average structure of CB7/MV showed a complete inclusion of the guest molecule, in harmony with earlier ^{1}H NMR spectroscopic experiments, in which the β aromatic protons of MV exhibited an upfield shift in the presence of the host. Moreover, irradiation of the methyne and methylene protons of CB7 gave rise to nuclear Overhauser effects for the α and β aromatic protons of MV.[24] These data could only be explained by the deep inclusion of the guest molecule in the cavity of CB7.[24] This

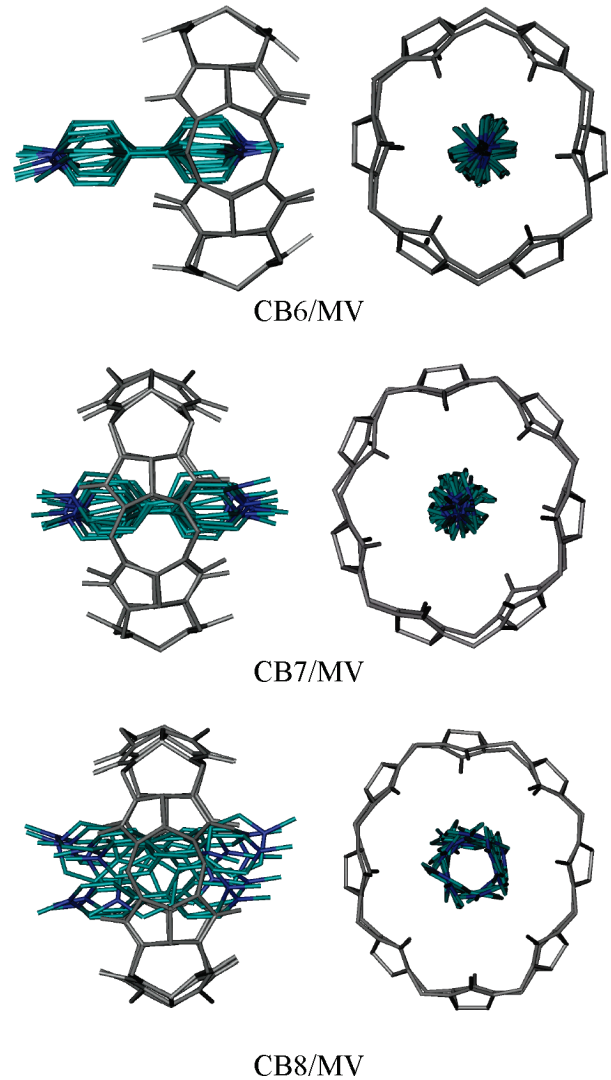

Figure 3. Dynamics of 1:1 complexes, shown as a clustered molecular display for CB/MV (side and top views).

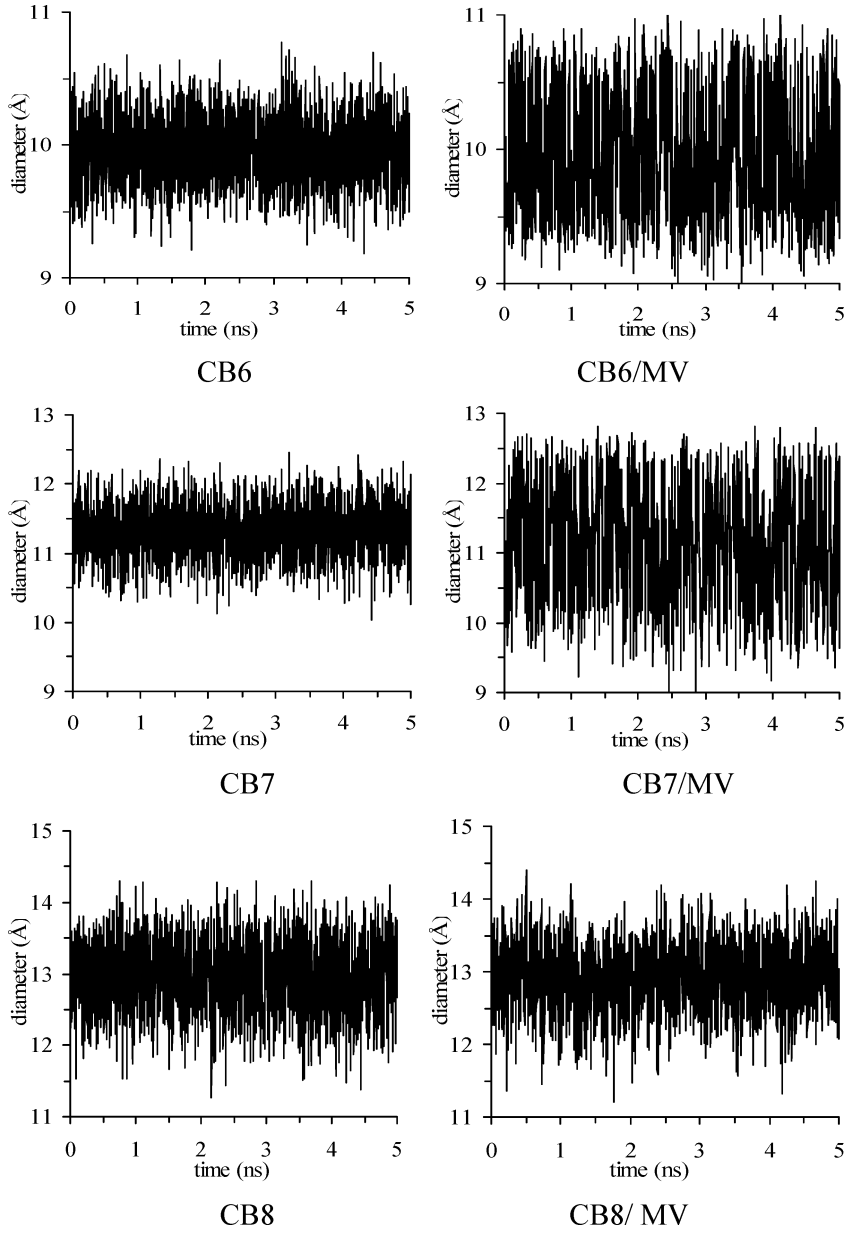

Figure 4. CB internal diameter as a function of simulation time.

structure reveals the favorable ion−dipole interaction between the positive charge on each end of the guest molecule and the portal oxygen atoms of CB7, while the hydrophobic part of the guest molecule was accommodated in the hydrophobic cavity. Similarly, CB8/MV average geometry also depicts complete inclusion. It seems that MV has more room inside the cavity because of the larger cavity size of CB8. Although the cavity of CB8 is large enough to accommodate two aromatic ring guest molecules, Kim and co-workers found that CB8 binds a single molecule of MV.[27,28]

The guest dynamics inside the host cavity, monitored by the superposition of 10 snapshots extracted from the MD trajectory for each complex, superimposed on a representative host structure, are given in Figure 3. A first assessment of the snapshots shows restricted translational movement of the guest in and out of the cavity in all CBs. This indicates the stability of the ion−dipole interaction in CB7 and CB8 during the simulations. The electrostatic potential of the CB cavity is negative,[2] which may explain the stable location of the cationic group of the guest molecule inside the CB6 cavity. Rotational motion of MV inside the cavity was observed in all complexes. Only in CB8 was the guest molecule found to translate within the cavity due to space availability.

Figure 4 shows the internal diameter (see scheme 1) values of CB6, CB7, and CB8 as a function of time in the absence and presence of the guest molecule. The MD averaged values and the corresponding standard deviations for the diameter are given in Table 1. Examining the standard deviations reveals that the fluctuation of the diameter increased upon complexation with MV in CB6 and CB7 but not in CB8. No noticeable change in the average value of the diameter upon inclusion of the guest molecule was observed for CB6 and CB8 (0.03 Å), but a change of 0.18 Å was measured for CB7. Free CB8 exhibits the largest fluctuation, while upon inclusion, CB7 fluctuates more.

Scheme 1. Perpendicular Internal Diameters Traced in MD Simulation

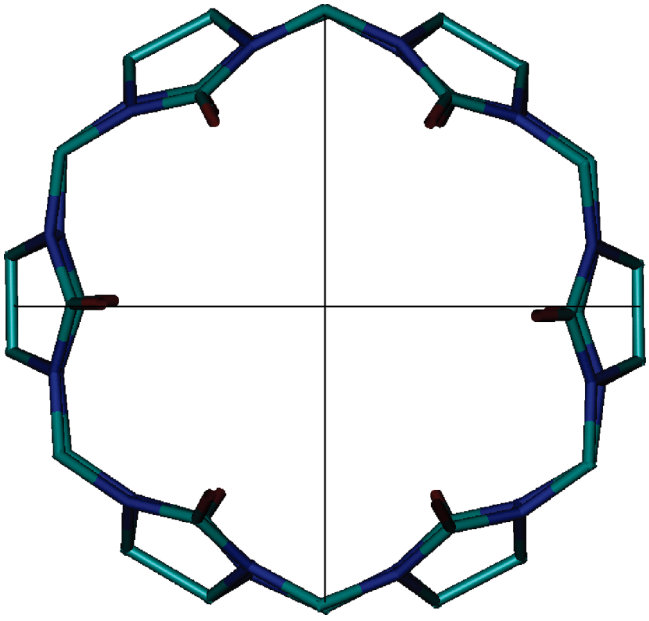

Table 1. MD-Averaged Values of the Internal Diameter of CB

complex	CB6	CB6/MV	CB7	CB7/MV	CB8	CB8/MV
average diameter (Å)	9.96	9.93	11.33	11.15	12.95	12.92
standard deviation (Å)	0.24	0.46	0.38	0.81	0.50	0.45

To better understand the conformational changes of the macrocyclic host upon guest inclusion, the values of two perpendicular internal diameters were traced in the MD simulation (Scheme 1). The absolute difference between the diameters as a function of simulation time and its distribution function for each system are given in Figure 5. Furthermore, the MD-averaged values and the corresponding standard deviations for the absolute difference are given in Table 2.

The difference between the diameters for CB6 shows a high probability around 0.2 Å for the free host. This value shifted to 0.8 Å in the complex. This indicates more sampling of a less symmetric structure than CB6 (oval shape) upon inclusion of the guest. The corresponding average value also increased after complexation (Table 2). This clearly demonstrates conformational changes of the macrocyclic structure induced by the guest inclusion. The situation is more dramatic in the case of CB7, upon whose inclusion, a severe broadening of the probability distribution peak was observed. The sampled structures for the complexed CB7 were found to span from 0 to 4 Å. The high extent of distortion in the case of CB7 (average value increased by ~230%) may be explained by the complete inclusion of the guest molecule in CB7, compared to partial inclusion in CB6. Inspection of the CB7/MV trajectory indicates that the rotation of the molecule inside the cavity induces a change in the diameter that passes the guest molecular plane (Figure 6). Figure 5 shows that CB8 exhibits more or less similar distortion before and after complexation, although complete inclusion of the guest molecule was found in accord with the higher cavity size compared to MV size.

Hydrogen Bond Analysis. A summary of the intermolecular hydrogen bonds that exist between each CB and the surrounding water molecules is presented in Table 3. For hydrogen bond analysis, a hydrogen bond cut distance $\leq$ 3.0 Å and an angle $\geq$ 120° were used. Results in Table 3 demonstrate, as expected, that the number of hydrogen bonds increases as the number of glycouril units increases. The portal oxygen atoms in the glycouril unit establish hydrogen bonds with the water molecules nearby, while the nitrogen atoms in CB do not play a role in the hydrogen bond network with the solvent. All complexes showed a reduction in the total number of hydrogen bonds upon complexation, indicating rearrangement of water molecules near both rims in the inclusion process.

MM/PBSA Results. Table 4 lists the binding free energies (kcal/mol) resulting from the MM/PBSA analysis of the 5 ns MD trajectories obtained for the studied complexes. Results show that the major contribution to the binding free energy is the host−guest electrostatic interactions (ΔE_{elec}), indicating the pronounced role of the ion−dipole interactions in such systems. CB7/MV shows the highest electrostatic contribution to the complex stability. This is expected since, unlike the CB6 complex, the two cationic groups interact with both carbonyl portals and associate in closer contact to the crowns than the CB8 complex does. van der Waals interactions (ΔE_{vdW}) were also found to be the highest in the CB7 complex. This is a direct result of the complete inclusion of the hydrophobic part of the guest molecule into the CB7 cavity accompanied by the fact that the guest has a better complementary size to the CB7 cavity than the CB8 does. The internal bonded interaction (ΔE_{INT}) values reflect significant conformational changes upon binding, especially in the CB6 system. The obtained ΔE_{INT} values are correlated well with the cavity size of the CB in which the values are getting more positive with decreasing the size of CB.

ΔG_{NP} values are negative for all complexes, indicating that the nonpolar surface term contributes positively to complex stability, though to a much lower extent when compared to the host−guest electrostatic and van der Waals interactions. Results also indicate unfavorable electrostatic solvation energy (positive values of ΔG_{PB}) evidenced by an overall positive value of the solvation free energy for all complexes. This is attributed to the reduction of contact area with the solvent of both host and guest molecules upon inclusion and hence less electrostatic interactions of the complexed molecules with the solvent than the free molecules. The resulting rank of ΔG_{PB} (or ΔG_{solv}) is expected, in which the CB7 complex exhibits the largest positive values, followed by CB8, and then CB6.

The computed binding free energies (ΔG) reveal that the tendency of MV to complex with CBs is in the order CB7 > CB8 > CB6, in agreement with the experimental trend.

NMODE calculations indicate that negative values of $T\Delta S_{conf}$ are obtained for all studied complexes, thus demonstrating a loss in the degrees of freedom upon binding. The $T\Delta S_{conf}$ value obtained for the CB8 complex is more negative (−13.5 kcal/mol) when compared to the expected

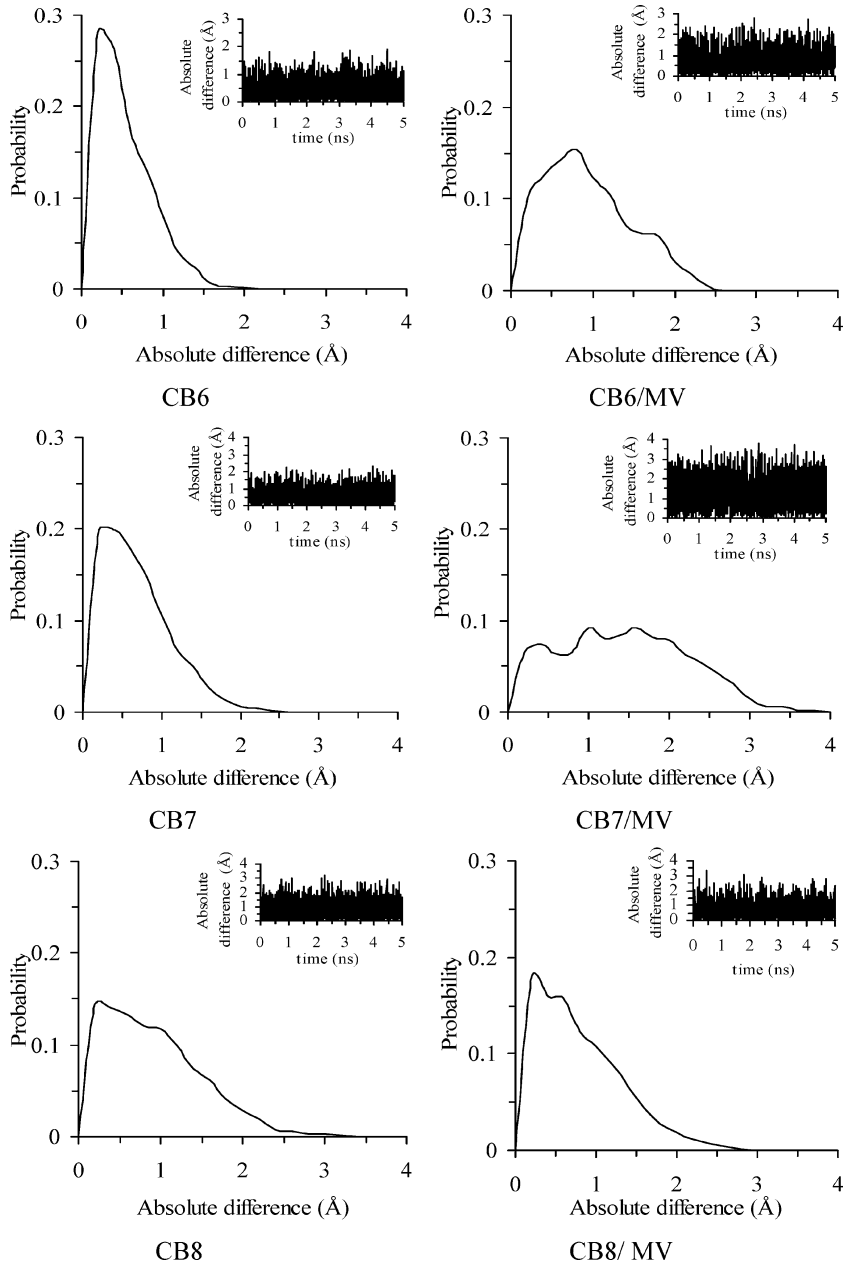

Figure 5. Distribution functions for the difference between two perpendicular internal diameters of CB. The difference as a function of simulation time is superimposed in each figure.

Table 2. MD-Averaged Values of the Absolute Difference between Two Perpendicular Internal Diameters of the Host

complex	CB6	CB6/MV	CB7	CB7/MV	CB8	CB8/MV
average difference (Å)	0.44	0.85	0.59	1.36	0.82	0.72
standard deviation (Å)	0.34	0.54	0.43	0.78	0.58	0.54

stiffer CB7 complex (−11.5 kcal/mol). The results are in contrast with the fact that the guest molecule has more room in the CB8 cavity than CB7, thus having more mobility in CB8, as can be seen in Figure 3. This might be attributed to the approximate nature of NMODE calculations. However, results in Tables 1 and 2 and Figures 4 and 5 show that the fluctuation of the diameter and the difference between the perpendicular diameters increased upon complexation with MV in CB7 but slightly decreased in CB8. This might explain the obtained $T\Delta S_{conf}$ values of CB7 and CB8 complexes.

It should be noted here that including the configurational entropy term in the binding free energy (ΔG^*) also gives a similar trend of MV desiring to complex with CBs.

Attempts to conduct MD simulation of MV with β-cyclodextrin (β-CD) prove that MV does not enter into the β-CD cavity since the guest molecule escapes from the β-CD cavity after a few hundred picoseconds. This is due to the presence of two cationic groups in the guest molecule, which interacts more with the surrounding water molecules. This also indicates that, although there is a similarity in the sizes of the hydrophobic cavities in CB7 and β-CD, the interaction at the cavity entrances with guest molecule in both systems is different.[25] This result is in accord with the experimental

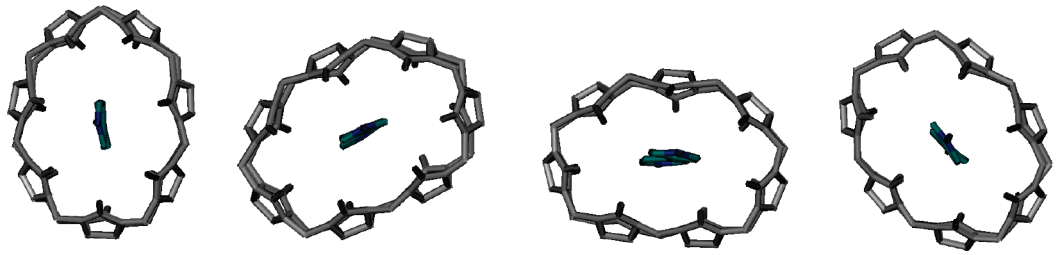

Figure 6. Extracted snapshots of the CB7/MV complex to show the effect of guest rotation on the diameter of the host molecule.

Table 3. Water−CB Intermolecular Hydrogen Bond Analysis for the Free and Complexed Host Molecules

HB/complex	CB6	CB6/MV	CB7	CB7/MV	CB8	CB8/MV
oxygen	8.13	5.67	9.68	7.33	10.36	9.53
nitrogen			0.02		0.01	0.01
total	8.13	5.67	9.70	7.33	10.37	9.54

Table 4. Binding Free Energies (kcal/mol) Resulting from MM/PBSA Analysis of the Studied Complexes[a]

	kcal/mol	CB6/MV	CB7/MV	CB8/MV
host	E_{elec}	−1033.7	−1118.3	−1378.2
	E_{vdW}	−34.0	−35.8	−36.9
	E_{INT}	257.6	303.1	350.7
	G_{NP}	4.4	5.2	6.0
	G_{PB}	−135.1	−167.7	−181.0
	G_{solv}	−130.7	−162.5	−175.0
	TS	81.7	94.5	107.2
guest	E_{elec}		142.7	
	E_{vdW}		12.7	
	E_{INT}		25.7	
	G_{NP}		2.1	
	G_{PB}		−160.6	
	G_{solv}		−158.5	
	TS		36.0	
complex	E_{elec}	−1003.1	−1118.1	−1360.0
	E_{vdW}	−46.5	−54.8	−47.9
	E_{INT}	289.0	330.6	375.7
	G_{NP}	4.6	4.9	6.0
	G_{PB}	−177.0	−170.9	−206.6
	G_{solv}	−172.4	−166.0	−200.6
	TS	98.7	119.0	129.7
Δ_{bind}	$-\Delta E_{elec}$	−112.1	−142.5	−124.5
	ΔE_{vdW}	−25.2	−31.7	−23.7
	ΔE_{INT}	5.7	1.8	−0.7
	ΔG_{NP}	−1.9	−2.4	−2.1
	ΔG_{PB}	118.7	157.4	135.0
	ΔG_{solv}[b]	116.8	155.0	132.9
	ΔG[c]	−14.8 (2.2)	−17.4(2.1)	−16.0 (1.8)
	$T\Delta S$	−19.0 (0.8)	−11.5 (0.7)	−13.5 (0.9)
	ΔG^*[d]	4.2 (2.4)	−5.9 (2.2)	−2.5 (2.0)
	ΔG_{expt}	−1.8[e]	−7.2[f]	−6.1[g], −6.9[h]

[a] Numbers in parentheses are standard deviations of the results. [b] $\Delta G_{solv} = \Delta G_{NP} + \Delta G_{PB}$ [c] $\Delta G = \Delta E_{elec} + \Delta E_{vdW} + \Delta E_{INT} + \Delta G_{NP} + \Delta G_{PB}$. [d] $\Delta G^* = \Delta G^b - T\Delta S_{conf}$ [e] Ref 24. [f] Ref 25. [g] Ref 27. [h] Ref 28.

data which showed that the β-CD/MV complex has a very low formation constant (∼0) with MV.[25] It is worth mentioning here the results of a recent MD study conducted by our group for the complexation of *N*-methyl-4-(*p*-methyl benzoyl)-pyridinium methyl cation with CB7 and β-CD. Results show that β-CD formed a more stable complex with the guest molecule than CB7 ($\Delta\Delta G \approx 1.9$ kcal/mol).[42] The guest molecule in that study possesses only one cationic site (methyl pyridinium cation), whereas MV has two cationic

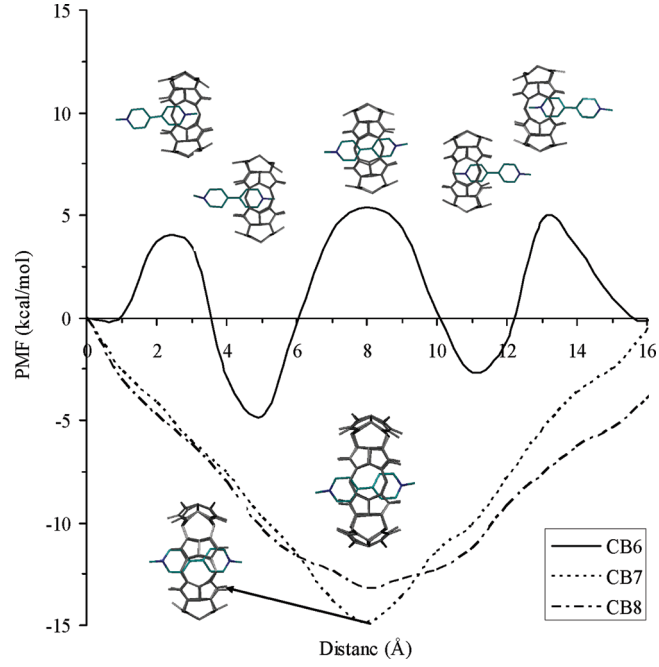

Figure 7. PMF profiles for inclusion of MV.

sites (two methyl pyridinium cations) capable of interacting with both CB7 portals by the favorable ion−dipole interactions, hence forming a more stable complex than β-CD. Moreover, the higher solubility of the dicationic guest compared to the monocationic guest is also responsible for a very small interaction with β-CD.

Umbrella Sampling (PMF Calculations). Figure 7 shows the results of PMF along the *r* coordinate (described in Figure 1). The PMF for the guest moving inside the CB6 cavity shows two minima at 5 and 11 Å with PMF values of −4.81 and −2.69 kcal/mol, respectively. Both minima correspond to more or less similar complex geometries which are composed of partial inclusion of the guest molecule. The difference in free energy between the two minima could be attributed to the distortion suffered by the macrocyclic compound when the guest passes from the unfavored complete inclusion to a partial inclusion, causing the difference in the free energy values. This is clear by the barrier existing at 8 Å which represents complete inclusion of the guest. The presence of the barrier explains the lack of sampling of snapshots composed of deep inclusion in the conventional MD simulation. There are also two barriers when the guest approaches both portals due to their small size. These barriers were not found for the bigger hosts, CB7

and CB8. The latter systems show only one minimum attributed to the complete inclusion geometry (8 Å).

Conclusion

The complexation of methyl viologen with cucurbit[*n*]urils was studied by molecular dynamics simulations, MM-PBSA and umbrella sampling. Deep inclusion of the guest was observed in CB7 and CB8 complexes, while partial inclusion occurs in the case of CB6. The CB macrocycle distorted upon inclusion of the guest molecule, and this was clear when the dimensions of the cavity and the guest molecule were close. MM-PBSA calculations revealed that host−guest electrostatic interactions were of major importance for the stability of the complexes. The movement of the guest molecule through the CB6 cavity involved energy barriers, while no barriers were found in CB7 and CB8 for the guest movement.

Acknowledgment. The authors wish to thank the Hashemite University and Yarmouk University for their financial support. The authors also wish to thank Lutfi Hussein and Heather Hoyt for revising the language of the manuscript.

References

(1) Rawashdeh, A. M.; Thangavel, A.; Sotiriou-Leventis, C.; Leventis, N. *Org. Lett.* **2008**, *10*, 1131.

(2) Lee, J. W.; Samal, S.; Selvapalam, N.; Kim, H.-J.; Kim, K. *Acc. Chem. Res.* **2003**, *36*, 621.

(3) Wang, R.; Macartney, D. H. *Tetrahedron Lett.* **2008**, *49*, 311.

(4) Lagona, J.; Mukhopadhyay, P.; Chakrabarti, S.; Isaac, L. *Angew. Chem., Int. Ed.* **2005**, *44*, 4844.

(5) Freeman, W. A.; Mock, W. L.; Shih, N. Y. *J. Am. Chem. Soc.* **1981**, *103*, 7367.

(6) Behrend, R.; Meyer, E.; Rusche, F. *Justus Liebigs Ann. Chem.* **1905**, *339*, 1.

(7) Kim, J.; Jung, I.-S.; Kim, S.-Y.; Lee, E.; Kang, J.-K.; Sakamoto, S.; Yamaguchi, K.; Kim, K. *J. Am. Chem. Soc.* **2000**, *122*, 540.

(8) Day, A. I.; Arnold, A. P.; Blanch, R. J.; Snushall, B. *J. Org. Chem.* **2001**, *66*, 8094.

(9) Day, A. I.; Blanch, R. J.; Arnold, A. P.; Lorenzo, S.; Lewis, G. R.; Dance, I. A. *Angew. Chem., Int. Ed.* **2002**, *41*, 275.

(10) Tuncel, D.; Steinke, J. H. G. *Chem. Commun.* **2001**, 253.

(11) Mock, W. L.; Pierpont, J. A. *J. Chem. Soc., Chem. Commun.* **1990**, 1509.

(12) Kornmüller, A.; Karcher, S.; Jekel, M. *Water Res.* **2001**, *35*, 3317.

(13) Jeon, Y. J.; Kim, S.-Y.; Ko, Y. H.; Sakamoto, S.; Yamaguchi, K.; Kim, K. *Org. Biomol. Chem.* **2005**, *3*, 2122.

(14) Wei, F.; Liu, S.-M.; Xu, L.; Cheng, G.-Z.; Wu, C.-T.; Feng, Y.-Q. *Electrophoresis* **2005**, *26*, 2214.

(15) Moch, W. L.; Shih, N. Y. *J. Org. Chem.* **1983**, *48*, 3618.

(16) Mezzina, E.; Cruciani, F.; Pedulli, G. F.; Lucarini, M. *Chem.—Eur. J.* **2007**, *13*, 7223.

(17) Choi, S. W.; Lee, J. W.; Ko, Y. H.; Kim, K. *Macromolecules* **2002**, *35*, 3526.

(18) Mock, W. L.; Shih, N. Y. *J. Am. Chem. Soc.* **1989**, *111*, 2697.

(19) Buschmann, H.-J.; Jansen, K.; Schollmeyer, E. *Acta Chim. Slov.* **1999**, *46*, 405.

(20) Li, Y.; Li, X.-Y.; Zhang, H.-Y.; Li, C.-J.; Ding, F. *J. Org. Chem.* **2007**, *72*, 3640.

(21) Sindelar, V.; Monn, K.; Kaifer, A. E. *Org. Lett.* **2004**, *6*, 2665.

(22) Sindelar, V.; Silvi, S.; Kaifer, A. E. *Chem. Commun.* **2006**, 2185.

(23) Zhang, H.; Paulsen, E. S.; Walker, K. A.; Krakowiak, K. E.; Dearden, D. V. *J. Am. Chem. Soc.* **2003**, *125*, 9284.

(24) Ong, W.; Gomez-Kaifer, M.; Kaifer, A. E. *Org. Lett.* **2002**, *4*, 1791.

(25) Kim, H.-J.; Jeon, W. S.; Ko, Y. H.; Kim, K. *Proc. Natl. Acad. Sci. U. S. A.* **2002**, *99*, 5007.

(26) Moon, K.; Kaifer, A. E. *Org. Lett.* **2004**, *6*, 185.

(27) Xiao, X.; Tao, Z.; Xue, S.-F.; Zhu, Q.-J.; Zhang, J.-X.; Lawrance, G. A.; Raguse, B.; Wei, G. *J. Inclusion Phenom. Macrocyclic Chem.* **2008**, *61*, 131.

(28) Jeon, W. S.; Kim, H.-J.; Lee, C.; Kim, K. *Chem. Commun.* **2002**, 1828.

(29) Frisch, M.; Trucks, G.; Schlegel, H.; Scuseria, G.; Robb, M.; Cheeseman, J.; Montagomery, J.; Verven, J. R.; Kudin, K.; Burant, J.; Millam, J. M.; Iyenger, S.; Tomasi, J.; Barone, V.; Mennucci, B.; Cossi, M.; Scalmani, G.; Rega, N.; Petersson, G.; Nakatsuji, H.; Hada, M.; Ehara, M.; Toyota, K.; Fukuda, R.; Hasegawa, J.; Ishida, M.; Nakajima, T.; Honda, Y.; Kitao, O.; Nakai, H.; Klene, M.; Li, X.; Konx, J.; Hratchian, H.; Cross, J.; Bakken, V.; Adamo, C.; Jaramillo, J.; Gomperts, R.; Stratmann, R.; Yazyev, O.; Austin, A.; Cammi. R.; Pomelli, C.; Ochterski, J.; Ayala, P.; Moromuka, K.; Voth, G.; Salvador, P.; Dannenberg, J.; Zakrzewski, V.; Dapprich, S.; Daniels, A.; Strain, M.; Farkas, O.; Malick, D.; Rabuck, A.; Raghavachari, K.; Foresman, J.; Ortiz, J.; Cui, Q.; Baboul, A.; Clifford, S.; Cioslwski, J.; Setvanov, B.; Liu, G.; Liashenko, A.; Piskorz, P.; Komaromi, I.; Marton, R.; Fox, D.; Keith, T.; Al-Laham, M.; Peng, C.; Nanayakkara, A.; Challacombe, M.; Gill, P.; Johnson, B.; Chen, W.; Wong, M.; Gonzalez, C.; Pople, J. *Gaussian 03*, Revision D.01; Gaussian, Inc.: Wallingford, CT, 2004.

(30) Bayly, C.; Cieplak, P.; Cornell, W.; Kollman, P. A. *J. Phys. Chem.* **1993**, *97*, 10269.

(31) Jakalian, A.; Bush, B. L.; Jack, D. B.; Bayly, C. I. *J. Comput. Chem.* **2000**, *21*, 132.

(32) Case, D. A.; Darden, T. A.; Cheatham, T. E.; Simmerling, C. L.; Wang, J.; Duke, R. E.; Luo, R. L.; Merz, K. M.; Wang, B.; Pearlman, D. A.; Crowley, M.; Brozell, S.; Tsui, V.; Gohlke, H.; Mongan, J.; Hornak, V.; Cui, G.; Beroza, P.; Schafmerister, C.; Caldwell, J. W.; Ross, W. S.; Kollman, P. A. *AMBER8*; University of California: San Francisco, CA, 2004.

(33) Wang, J.; Wolf, R. M.; Caldwell, J. W.; Kollman, P. A.; Case, D. A. *J. Comput. Chem.* **2004**, *25*, 1157.

(34) Jorgensen, W. L.; Chandrasekhar, J.; Madura, J. D.; Impey, R. W.; Klein, M. L. *J. Chem. Phys.* **1983**, *79*, 926.

(35) Darden, T.; York, D.; Pederson, L. *J. Chem. Phys.* **1993**, *98*, 10089.

(36) Humphrey, W.; Dalke, A.; Schulten, K. *J. Mol. Graphics* **1996**, *14*, 33.

(37) Sanner, M. F.; Olson, A. J.; Spehner, J. C. *Biopolymers* **1996**, *38*, 305.

(38) Hou, T. J.; Guo, S. L.; Xu, X. J. *J. Phys. Chem. B* **2002**, *106*, 5527.

(39) El-Barghouthi, M. I.; Jaime, C.; Al-Sakhen, N. A.; Issa, A. A.; Abdoh, A. A.; Al-Omari, M. M.; Badwan, A. A.; Zughul, M. B. *THEOCHEM* **2008**, *853*, 45.

(40) Kumar, S.; Rosenberg, J. M.; Bouzida, D.; Swendsen, R. H.; Kollman, P. A. *J. Comput. Chem.* **1992**, *13*, 1011.

(41) Souaille, M.; Roux, B. *Comput. Phys. Commun.* **2001**, *135*, 40.

(42) Rawashdeh, A. M.; El-Barghouthi, M. I.; Assaf, K. I.; Al-Gharabli, S. I. *J. Inclusion Phenom. Macrocyclic Chem.* **2009**, *64*, 357.

CT900622H